Characterization and quantification of endogenous fatty acid nitroalkene metabolites in human urine

Sonia R. Salvatore, Dario A. Vitturi, Paul R.S. Baker, Gustavo Bonacci, Jeffrey R. Koenitzer, Steven R. Woodcock, Bruce A. Freeman* and Francisco J. Schopfer*

Department of Pharmacology & Chemical Biology, University of Pittsburgh, Pittsburgh, PA 15261, USA;

Running title: Detection of nitrated conjugated linoleic acid in urine

*Correspondence: Bruce A. Freeman PhD or Francisco J. Schopfer PhD, Department of Pharmacology and Chemical Biology, University of Pittsburgh, E1340 BST, 200 Lothrop St., Pittsburgh, PA, 15261, USA. Phone: 412-648-9319; Fax: 412-648-2229; Email: freerad@pitt.edu or fjs2@pitt.edu

ABSTRACT

The oxidation and nitration of unsaturated fatty acids transforms cell membrane and lipoprotein constituents into mediators that regulate signal transduction. The formation of 9-NO_2-octadeca-9,11-dienoic acid and 12-NO_2-octadeca-9,11-dienoic acid stems from peroxynitrite- and myeloperoxidase-derived nitrogen dioxide reactions as well as secondary to nitrite disproportionation under the acidic conditions of digestion. Broad anti-inflammatory and tissue-protective responses are mediated by nitro-fatty acids. It is now shown that electrophilic fatty acid nitroalkenes are present in the urine of healthy human volunteers (9.9 ± 4.0 pmol/mg creatinine); along with electrophilic 16- and 14-carbon nitroalkenyl β-oxidation metabolites. High resolution mass determinations and co-elution with isotopically-labeled metabolites support renal excretion of cysteine-nitroalkene conjugates. These products of Michael addition are in equilibrium with the free nitroalkene pool in urine and are displaced by thiol reaction with $HgCl_2$. This reaction increases the level of free nitroalkene fraction >10-fold and displays a K_D of 7.5×10^{-6} M. In aggregate, the data indicates that formation of Michael adducts by electrophilic fatty acids is favored under biological conditions and that reversal of these addition reactions is critical for detecting both parent nitroalkenes and their metabolites. The measurement of this class of mediators can constitute a sensitive non-invasive index of metabolic and inflammatory status.

INTRODUCTION

Nitro-fatty acid derivatives are formed during both gastric acidification and by the array of oxidative inflammatory reactions that nitric oxide ($^{\cdot}$NO) and nitrite (NO_2^-) undergo to induce nitrogen dioxide ($^{\cdot}NO_2$)-dependent biomolecule nitration (1). Nitroalkene substituents are electrophilic and promote Michael addition of fatty acids with biological nucleophiles such as cysteine and histidine. The extent, rate and reversibility of these reactions will be dictated both by the concentration and reactivity of individual nucleophiles. In this regard, protein structure and compartmentalization affect the reactivity of individual nucleophilic centers and will define the molecular targets of electrophilic fatty acids.

While enzymatically-oxygenated unsaturated fatty acids typically transduce anti-inflammatory actions via specific g protein-coupled receptor (GPCR) ligand activity (2, 3), transcriptional responses to electrophilic fatty acids reveal that a broader array of signaling events are instigated (4, 5). The basis for this pleiotropy resides in the facile Michael addition of electrophilic fatty acid derivatives with nucleophilic centers of proteins that regulate structure and function (6). Functionally-significant protein targets of electrophilic fatty acids include the transcriptional regulatory protein complex nuclear factor kappa B (NFkB), the Kelch-like ECH-associated protein 1 (Keap1) regulator of nuclear factor (erythroid-derived-2)-like 2 (Nrf2), heat shock factor-1 (HSF-1), peroxisome proliferator-activator receptor-γ (PPARγ) and histone deacetylases (HDAC) (7). These transcriptional regulatory proteins contribute to the control the expression of hundreds of genes that include cytokines, antioxidant enzymes, heat shock response proteins and enzymes of intermediary metabolism (4, 5, 8-14).

Conjugated 9,11-linoleic acid appears to be the preferred endogenous substrate for metabolic and inflammatory-mediated fatty acid nitration. This is attributed to its clinical abundance and the high reactivity to addition reactions of the external flanking carbons of conjugated dienes, as opposed to monoalkenes or bis-allylic dienes (1). Once formed, electrophilic nitro fatty acids (NO_2-FA) can undergo addition to glutathione (GSH), enzymatic reduction to a non-electrophilic nitroalkene and β-oxidation (15, 16). GSH nitroalkylation products are exported from cells as GSH conjugates by multidrug resistant proteins (MRP)(15). In turn, GSH-NO_2-FA conjugates may also be metabolized by peptidases to cysteinylglycine and cysteine conjugates, N-acetylated and excreted via renal or biliary mechanisms.

Herein, we identify the two principal nitro derivatives of conjugated linoleic acid, 9-nitro-octadeca-9,11-dienoic acid and 12-nitro-octadeca-9,11-dienoic acid, in the urine of healthy humans. Electrophilic 16-, 14- and 12-carbon β-oxidation metabolites and their corresponding cysteinyl-conjugates were also detected. Structural characterization and quantification via high resolution mass spectrometry was guided by the comparison of endogenous metabolites to both synthetic 9- and 12-$^{15}NO_2$-CLA, and the products of $^{15}NO_2$-CLA metabolism by isolated and perfused rodent heart. Notably, the detectable concentrations of fatty acid nitroalkenes and corresponding cysteine conjugates in human urine were strongly influenced by a chemical equilibrium induced by thiol availability and pH. The formation, protein adduction, metabolism and excretion of electrophilic fatty acids constitute a metabolic network capable of regulating steady-state levels and activity of these molecules under basal non-pathological conditions.

Inasmuch as fatty acid nitration is influenced by the dietary, metabolic and inflammatory status of organisms, the present data also provides an approach and perspective for non-invasively detecting the magnitude of redox reactions stemming from metabolism and products of partially reduced oxygen species, ˙NO and NO_2^-.

EXPERIMENTAL PROCEDURES

Materials - (9Z,11E)-octadeca-9,11-dienoic (9,11-CLA, referred as conjugated linoleic acid, CLA) was purchased from Nu-Check Prep (Elysian, MN). [$^{13}C_{18}$] (9Z,12Z)-octadeca-9,12-dienoic acid and [$^{13}C_{18}$] (9Z)-octadeca-9-enoic acid (> 98% isotopic purity) and Na [$^{15}N]O_2$ were purchased from Cambridge Isotope Laboratories, Inc. (Andover, MA). NO_2-OA, NO_2-LA, NO_2-[$^{13}C_{18}$]LA, NO_2-[$^{13}C_{18}$]OA were synthesized as previously (17-19). NO_2-CLA and $^{15}NO_2$-CLA were synthesized by acidic nitration of (9Z,11E)-CLA with either [^{14}N]nitrite or [^{15}N]nitrite as previously (1). Specific 9-NO_2-CLA and 12-NO_2-CLA were synthesized de novo and their chemical characterization will be separately reported. $NaNO_2$ and β-mercaptoethanol (BME) were obtained from Sigma/Aldrich (St Louis, MO). Solvents used for synthetic reactions were of HPLC grade or better from Fisher Scientific (Fairlawn, NJ). Solvents used for extractions and mass spectrometric analyses were from Burdick and Jackson (Muskegon, MI). Solid phase extraction columns (SPE, C-18 reverse phase; 500 mg, 6 ml capacity) were purchased from Thermo Scientific.

Chromatography - Fatty acid nitration products in lipid extracts were analyzed by HPLC-ESI MS/MS using gradient solvent systems consisting of H_2O containing 0.1% acetic acid (solvent A) and acetonitrile containing 0.1% acetic acid (solvent B). Lipid extracts were resolved for quantitation using a reverse phase HPLC column (2 x 20 mm C18 Mercury column; Phenomenex) at a 0.75 ml/min flow rate. Samples were applied to the column at 11% B (1 min) and eluted with a linear increase in solvent B (11%-100% B in 9 min). Characterization analysis to identify structural isomers and metabolites was performed using an analytical C18 Luna column (2 x 150 mm, 3 μm particle size, Phenomenex) at a 0.25 ml/min flow rate. Samples were resolved using the following gradient program: 0-1 min, 45% solvent B; 1-45 min, from 45 to 80% solvent B; 45-46 min, from 80 to 100% solvent B. BME adduct analysis was performed on an analytical C18 Luna column (2 x 100 mm, 5 μm particle size, Phenomenex) at a 0.75 ml/min flow rate. Samples were resolved using the following gradient program: 0.5-3 min, from 5-35% solvent B; 3-15 min from 35-100% solvent B.

Mass spectrometry - Analytes of interest were characterized both in CID and HCD mode using an LTQ Velos Orbitrap (Velos Orbitrap, ThermoScientific) equipped with a HESI II electrospray source. The following parameters were used: source temperature 400 °C, capillary temperature 360 °C, sheath gas flow 30, auxiliary gas flow 15, sweep gas flow 2, source voltage -3.3 kV, S-lens RF level 44 (%). The instrument FT-mode was calibrated using the manufacturers recommended calibration solution with the addition of malic acid as a low m/z calibration point in the negative ion mode. Analyte quantification was performed in multiple reaction monitoring mode (MRM) using an AB5000 or a API4000 Qtrap triple quadrupole mass spectrometer (Applied Biosystems; San Jose, CA) equipped with an electrospray ionization source. Internal standard curves using synthetic NO_2-CLA and $^{15}NO_2$-CLA were prepared using human urine as matrix to quantify endogenous nitrated fatty acids. Precursor ion scans were performed to identify any other eluting lipids losing a nitro group (*m/z* 46) upon CID.

Lipid extraction from urine - Urine samples (first void of the day) were collected from healthy human volunteers (University of Pittsburgh IRB PRO07110032 or 0905750B-7) and either stored at -80°C (<1 month) or extracted immediately, with no significant differences in either lipid profile or concentrations observed under these conditions. For experiments studying the reversibility of nitroalkene-cysteine reactions, urine was incubated with 10 mM $HgCl_2$ for 30 min at 37°C before lipid extraction. Urinary fatty acids and Michael addition products were extracted using C-18 SPE columns. Columns were conditioned with 100% methanol (MeOH), followed by 2 column volumes of 5% MeOH. For clinical samples, internal standards NO_2-[$^{13}C_{18}$]LA, NO_2[$^{13}C_{18}$]-OA and or $^{15}NO_2$-CLA were added to 1-3 ml urine containing 5% MeOH (1.8 pmol/ml final concentration); vortexed and equilibrated at 4 °C for 5 min prior to extraction. Samples were loaded into the SPE column and washed with 2 column volumes of 5% MeOH and the column was dried under vacuum for 30 min. Lipids were eluted with 3 ml MeOH, solvent was evaporated, and samples were dissolved in MeOH for analysis by HPLC-electrospray ionization mass spectrometry (ESI MS/MS). Nitro-fatty acid levels were normalized to urine creatinine concentrations that were determined using a colorimetric assay measuring absorbance at 535 nm after dilution in NaOH and reaction with picric acid (20).

Generation of cysteine and mercapturic acid conjugate standards - Synthetic standards were generated by the reaction of 200 mM N-acetyl-cysteine with 100 µM NO_2-CLA or 100 µM $^{15}NO_2$-CLA in 50 mM phosphate buffer pH 8 at 37 °C for 3 h. The lipid conjugates were loaded on a C-18 SPE column pre equilibrated with 5% MeOH and then eluted with MeOH. Mass spectrometric structural analysis of cysteinyl- and N-acetyl-cysteinyl-conjugates (mercapturates) was performed in both negative and positive ion mode using accurate mass determinations and respective MRMs.

Generation of NO_2-CLA metabolites by Langendorff-perfused hearts – Hearts from male Sprague-Dawley rats (Harlan lab, Indianapolis, IN, USA) were isolated and perfused (at 8-10 ml/min) in a Langendorff system as previously (21). Hearts were stabilized for 30 min and then $^{15}NO_2$-CLA (10 mM in methanol) was introduced to the perfusate at 10 µl/min. NO_2-CLA was dissolved in methanol because of poor solubility in aqueous milieu. The use of albumin to stabilize and solubilize NO_2-CLA in buffer was avoided because of alternative reactions with protein cysteine and histidine residues. The effluent was collected and metabolites recovered after solid phase extraction. Labeled cysteinyl conjugates were synthesized by reacting fractions containing $^{15}NO_2$-CLA metabolites with cysteine (100 µM) in 50 mM KH_2PO_4 buffer pH 8 for 3 h. All animals were housed in accordance with the Guide for the Care and Use of Laboratory Animals published by the US National Institutes of Health (NIH Publication No. 85-23, revised 1996) and all animal studies were approved by the University of Pittsburgh Institutional Animal Care and Use Committee (approval 12070398).

Determination of equilibrium constants by UV-visible spectral deconvolution – The reaction of cysteine with NO_2-OA in 20 mM sodium phosphate buffer at pH 7.4, was monitored by UV-visible spectroscopy. Briefly 50-85 µM NO_2-OA was reacted with 0.5-10-fold excess cysteine at 25°C until spectral changes were no longer observed. Resulting concentrations of free NO_2-OA, free cysteine and Cys-NO_2-OA adducts were determined by spectral deconvolution analysis (22). Equilibrium constants were obtained by non-linear regression analysis adjusting to a one-site specific binding model using GraphPad Prism 5.0. Reference spectra for cysteine, NO_2-OA and Cys-NO_2-OA were acquired between 220 and 400 nm and extinction coefficients were obtained at each wavelength. Cys-NO_2-OA was generated by reacting 35 µM NO_2-OA with excess cysteine (3mM) at pH 7.4 and subtracting the contribution of the thiolate absorbance to the final spectrum.

RESULTS

Conjugated linoleic acid nitration products in human urine. Free and protein-adducted NO_2-CLA regioisomers were detected in human plasma generated by inflammatory, metabolic and proton-catalyzed reactions in the gastric compartment (1). This motivated the analysis of NO_2-CLA regioisomers and their metabolites in human urine as a non-invasive approach for determining the endogenous production and reactions of these species. LC-ESI-MS/MS analysis of urine using MRM 324.2/46 (m/z corresponding to NO_2-CLA and the formation of the NO_2^- anion upon CID) presented two well-defined chromatographic peaks that co-eluted with synthetic 9-$^{15}NO_2$-CLA and 12-$^{15}NO_2$-CLA (**Fig 1a-c**). These molecular ions displayed retention times that were intermediate between NO_2-[$^{13}C_{18}$]LA (bis-allylic LA, shorter retention time) and NO_2-[$^{13}C_{18}$]OA (longer retention time) (**Fig 1d,e**).

Quantification of conjugated diene-containing fatty acid nitration products in human urine. Levels of NO_2-CLA in human urine were measured in the MRM scan mode using $^{15}NO_2$-CLA as an internal standard to correct for losses due to extraction. The content of NO_2-CLA in urine was 9.97 +/- 3.98 pmol/mg creatinine, with up to 100-fold differences in basal NO_2-CLA concentrations in different healthy volunteers (0.5 to 42.6 pmol/mg creatinine, **Suppl. Table 1**).

Electrophilic β-oxidation products of NO_2-CLA in urine. Mitochondrial β-oxidation of synthetic NO_2-OA occurs in mice following intravenous injection (16). In order to evaluate if endogenous NO_2-CLA β-oxidation metabolites could be detected in human urine, a sequential scan for precursor ions of 46 (NO_2^-) with mass losses of 28 amu (C_2H_4) from the parent NO_2-CLA was performed. Chromatographic peaks corresponding to dinor-NO_2-CLA (m/z 296.2, 1 round of β-oxidation) and tetranor-NO_2-CLA (m/z 268.2, 2 rounds of β-oxidation) ion precursors were detected (**Fig 2a**).

Fatty acid nitration yields electrophilic nitroalkene derivatives that undergo conjugate addition with low and high molecular weight thiols. To test the electrophilic nature of these newly-identified urinary fatty acid nitration products, 500 mM of β-mercaptoethanol (BME) was added to urine samples for 2 h and products were determined by LC-MS/MS after extraction (**Fig 2**). After BME addition, all species previously identified as nitrated fatty acids were transformed into the corresponding BME addition products and no longer detected at their original retention times (**Fig 2b,** structures shown in **2d**). Peaks co-eluting with BME adducts (**Fig. 2b-c**) that displayed the m/z of non-adducted species (**Fig. 2c**) provided additional diagnostic insight. These peaks reflected in-source fragmentation products due to the neutral loss of BME (β elimination reaction) during adduct ionization (23). This indicated the electrophilic nitroalkene configuration of both urinary NO_2-CLA and its β-oxidation products, with no other additional hydroxy-, oxo- or non-electrophilic nitroalkane-containing derivatives of NO_2-CLA detected in urine (data not shown).

High resolution mass spectrometry comparison of NO_2-CLA β-oxidation products in urine and NO_2-CLA metabolites formed by isolated and perfused rat hearts. The addition of nitrated fatty acids to the perfusate of Langendorff rat heart preparations yielded corresponding β-oxidation derivatives in the effluent. Thus, $^{15}NO_2$-CLA was infused into isolated rat hearts in order to generate isotopically-labeled standards for characterizing putative NO_2-CLA products in human urine. Accurate mass determinations at the 2 ppm level confirmed the atomic composition of the different NO_2-CLA metabolites proposed for both human urine and cardiac $^{15}NO_2$-CLA metabolic products (**Fig 3, Table 1**). This high resolution MS/MS analysis also gave fragmentations that defined these products as 12-NO_2-hexadeca-9,11-dienoic acid, 9-NO_2-hexadeca-

6

9,11-dienoic acid, **(Fig 3a, Suppl Fig 1a)** 10-NO_2-hexadeca-7,9-dienoic acid, 7-NO_2-hexadeca-7,9-dienoic acid (dinor NO_2-CLAs) **(Fig 3b, Suppl Fig 1b)**, 8-NO_2-hexadeca-5,7-dienoic acid and 5-NO_2-hexadeca-5,7-dienoic acid (tetranor NO_2-CLAs) c) **(Fig 3c, Suppl Fig 1c)**, for both human urine and rodent heart metabolites (See Table 1 for product ion identification). The chromatographic profile of these nitrated fatty acid species correlated between the two sources, supporting the notion that NO_2-CLA undergoes β-oxidation and that these products are present in the urine of healthy humans. Whereas the retention times for the different dinor-NO_2-CLA isomers were identical, there were differences in the relative ion intensities of particular metabolites generated by cardiac perfusion and present in urine **(Fig 3b, peaks 1 and 2)**. The urine of different subjects presented a strong correlation (R>0.94) between the levels of NO_2-CLA and its β-oxidation products (dinor- and tetranor-NO_2-CLA) **(Fig. 4)**, supporting that these 16- and 14- carbon nitroalkenes all shared NO_2-CLA as the precursor.

Detection and characterization of cysteinyl-nitro-fatty acid conjugates in urine. Sequential addition to GSH, export to the extracellular space via MRPs and peptidase-mediated cleavage is a potential *in vivo* route for the metabolic disposition of nitro-fatty acids (15). Cysteine conjugates of NO_2-CLA were detected in human urine, affirmed by co-elution with the synthetic internal standard Cys-$^{15}NO_2$-CLA **(Fig 5a)**. Positive ion mode analysis of ^{15}N-labeled synthetic and endogenous Cys-NO_2-CLA **(Fig 5c)** revealed a characteristic primary neutral loss of HNO_2, with secondary losses of CO_2, H_2O and fragmentation of the amino acid side chain **(Fig 5b, Suppl Fig 2a, Suppl. Scheme 1)**. This was further confirmed by fragmentation of both endogenous and synthetic Cys-NO_2-CLA following the neutral loss of NO_2-CLA in the negative ion mode **(Suppl Fig 2b)**.

The presence of 16 and 14 carbon electrophilic NO_2-CLA metabolites in urine suggested that these derivatives might also form cysteine conjugates. The presence of Cys-dinor-NO_2-CLA, Cys-tetranor-NO_2-CLA and Cys-hexanor-NO_2-CLA in human urine was evaluated by MS/MS in the negative and positive ion mode. In the negative ion mode, the fragmentation of these addition products is characterized by neutral losses of the nitrated fatty acid and cysteine moiety, albeit the latter is less prevalent. Selective reaction monitoring of the neutral loss of the nitroalkene precursor led to the detection of addition products containing 16, 14 and 12 carbon long nitro-fatty acids **(Suppl Fig 2b).** In order to confirm the identity of these metabolites, cysteine-conjugated standards were prepared from $^{15}NO_2$-CLA β-oxidation metabolites obtained from isolated and perfused rat hearts. The retention times and peak patterns obtained from heart-derived metabolites closely matched those obtained from urine samples **(Fig 5a)**. The peak multiplicity observed both in rodent heart and human urine samples likely results from the different isomeric configurations that nitroalkenes can adopt upon successive cycles of cysteine addition and release. Finally, the atomic composition of all metabolites was confirmed by high resolution mass analysis **(Suppl Fig 2c)**. Importantly, fragmentation analysis of cysteine adducts yielded the canonical neutral loss of HNO_2, a hallmark for nitro-containing fatty acids including nitroalkylated peptides, bisallylic and mono-unsaturated nitroalkenes and NO_2-CLA **(Fig 5b inset)**(14, 17, 24).

The presence of mercapturate-NO_2-CLA conjugates in human urine was evaluated by producing a synthetic standard from the reaction of N-acetyl-cysteine with $^{15}NO_2$-CLA. Mass spectrometric analysis indicated that these compounds fragment in the negative ion mode with neutral losses of the conjugated fatty acid. Single reaction monitoring of urine revealed that these species were detectable at trace levels not warranting or allowing further characterization.

7

Reversibility of Michael addition by NO$_2$-CLA. LC-MS analysis of cysteine adducts of NO$_2$-CLA in human urine indicates that these metabolites are present as a mixture of isomers, suggesting that cysteine addition to nitroalkenes is a reversible process under physiological conditions. To test this hypothesis, the stability of Cys-^{15}NO$_2$-CLA was analyzed in a human urine matrix and in methanol. When Cys-^{15}NO$_2$-CLA was added to methanol at 37 °C for 2 h there was no formation of free [^{15}N]O$_2$-CLA, in agreement with limited reversibility of Michael additions in organic solvents. In contrast, when Cys-^{15}NO$_2$-CLA was added to freshly-obtained urine at 37°C, a chemical equilibrium was established and non-alkylated ^{15}NO$_2$-CLA was evident **(Fig 6a-b)**. Expanding on this insight, human urine was treated with the thiol-reactive Lewis acid HgCl$_2$. The reaction of HgCl$_2$ (10 mM) for 30 min at 37 °C promoted the release of free nitroalkenes, concomitant with the complete loss of the cysteine-conjugates. Similar results were obtained with different chain length nitro-fatty acid metabolites **(Fig 7)**.

Equilibrium constant of the NO$_2$-FA reaction with cysteine. To better define the reversibility of thiol addition to reactive nitroalkenes, the equilibrium constant for the reaction between cysteine and NO$_2$-OA was determined. Nitro-oleic acid is a prototypic nitroalkene for which reaction rates with GSH have been characterized (25) . The formation of Cys-NO$_2$-OA was monitored by UV-visible spectroscopy and analyzed by non-linear deconvolution **(Fig 8a)**. NO$_2$-OA was incubated with increasing concentrations of cysteine thiolate and the relative concentrations of free and adducted nitroalkene were determined by spectral deconvolution **(Fig 8b)**. Finally, a dissociation constant ($K_D = 7.5 \times 10^{-6}$ M) was derived by fitting fractional lipid binding values obtained at increasing concentration of added thiolate to a one-site hyperbolic binding model **(Fig 8c)**.

8

DISCUSSION

The initiation, propagation and resolution phases of inflammation are regulated in part by enzymatically- and non-enymatically-derived fatty acid oxidation products. These include isoprostanes (26), neuroprostanes (27), prostaglandins, and both oxo- and hydroxyl- derivatives of arachidonic, eicosapentaenoic and docosahexaenoic acids (28). The detection of several of these mediators in urine and plasma has enabled their use as clinically-significant and validated markers of disease progression, such as the isoprostane products of oxidative and inflammatory reactions (29, 30). This motivates the further identification and characterization of redox-derived lipid metabolites in urine that might shed light on the physiological and pathophysiological reactions of various oxides of nitrogen. Fatty acid nitroalkene derivatives are produced via reactions associated with inflammation, metabolic acidosis, and gastric acidification. Free and esterified nitro-fatty acid derivatives have been detected in human and animal plasma, low density lipoproteins, inflammatory mediator-activated macrophages and rodent heart and isolated cardiac mitochondria after ischemia and reperfusion (14, 17, 31-33).

NO_2-CLA isomers are endogenously formed by nitration of the flanking conjugated diene carbons (C9 and C12) of (9Z,11E)-octadeca-9,12-dienoic acid. (1). These nitration products are present in human plasma and herein we report their presence is reported in healthy human urine. In addition to parent nitroalkene derivatives, these species are accompanied by their β-oxidation products and corresponding cysteine adducts. Notably, the cysteine Michael addition products of NO_2-CLA and related metabolic products exist in equilibrium with the free nitroalkene derivatives (Figs. 7 and 8).

The detection and quantification of fatty acid nitroalkenes is complicated by their facile Michael addition reactions and metabolism (4, 24). Consequently, the concentrations of fatty acid nitration products in tissues and fluids have been the subject of controversy (34). Initial concentrations of free and esterified NO_2-FA were initially reported to be in the high nM range (14). Subsequent studies support that 9-NO_2-OA and 10-NO_2-OA are present in the free form in plasma at concentrations of approximately 1 nM (33). In line with this, 9-NO_2-CLA and 12-NO_2-CLA are the most abundant linoleic acid-derived nitrated species that have been detected at present, with plasma concentrations of the free fatty acid adduct also approaching 1 nM in healthy human donors (1).

The presence of NO_2-CLA and its derivatives in human urine samples was confirmed by comparison with corresponding ^{15}N-labeled standards, as well as by high resolution MS analysis. While the levels of NO_2-CLA, dinor-NO_2-CLA and tetranor-NO_2-CLA were similar in human urine (Fig 4), the concentration of hexanor-NO_2-CLA was considerably lower. This contrasts with the metabolite profile obtained from NO_2-CLA-perfused rat hearts, where the levels of dinor-NO_2-CLA were lower than those of NO_2-CLA and tetranor-NO_2-CLA. This indicates either species-specific differences in metabolism or an intrinsic inability of dinor-NO_2-CLA to escape the β-oxidation cycle in heart tissue. Thus, the endogenous formation of dinor-NO_2-CLA most likely stems from non-cardiac tissues. Moreover, the isomeric composition of dinor-NO_2-CLA from rat heart is different from that observed in human urine. The multiplicity of peaks detected in cardiac venous outflow may be a result of conjugated diene stereoisomerization after Michael addition to, and then release from, nucleophilic targets.

9

The Michael addition of nitroalkenes to GSH has been reported in plasma, tissues and cells in culture (24). These products are preferentially formed intracellularly via non-enzymatic conjugation in a compartment where GSH concentrations are ~6 mM, (15, 35). In this regard, glutathione–S-transferases (GSTA1-1, A4-4, M1a-1a, and P1a-1a) do not participate in GSH conjugation of nitrated linoleic and oleic acid (35). Inactive GSH conjugates are then exported to the extracellular milieu through MRPs to enter the circulation (15) and processed by hepatic γ-glutamyl transpeptidases and renal dipeptidases to yield cysteine conjugates analogous to those of leukotriene metabolism (36-38). Thus, a comprehensive detection of electrophilic lipid metabolites in the urine also encompasses cysteine and mercapturate conjugates, as for isothiocyanates (39). Human urine revealed higher levels of nitroalkene-cysteine conjugates, compared with free fatty acid or mercapturic acid derivatives. Although mercapturates are typically in greater concentrations than cysteine conjugates in urine, this observation is not uncommon, as leukotriene E4 levels are 9-fold greater than those of its N-acetyl derivatives (40).

Both free and protein tyrosine, and to a lesser extent tryptophan, are nitrated by the same reactions that yield fatty acid nitration products (1, 41). Post-translational protein nitration and the neoepitopes that it generates are viewed as both indices and mediators of pathogenic oxidative inflammatory reactions (42). Notably, tyrosine does not compete with CLA for nitration and might even promote NO_2-CLA generation (1). The consideration of plasma and urinary endogenous fatty acid nitroalkenes is relevant beyond a role as biomarkers of oxidative nitration reactions, since these species also potently mediate signaling reactions that limit inflammation. Potential mechanisms underlying these actions include a) inhibition of neutrophil function and platelet activation (43, 44), b) serving as partial agonists for PPARγ (14, 15, 45-47), c) inhibition of cytokine expression via inhibition of DNA binding by the p65 unit of NF-κB (48) and d) up-regulation of phase 2 gene expression via Keap1/Nrf2-dependent (5, 49, 50) and -independent mechanisms (51). Critical pro-inflammatory enzymatic activities are also inhibited by fatty acid nitroalkenes, including xanthine oxidoreductase and cyclooxygenase-2 (52, 53). These actions result in anti-inflammatory responses in diverse animal models of disease including limiting restenosis after vessel injury (54), attenuation of weight gain and loss of insulin sensitivity in murine models of metabolic syndrome (6, 55), inhibition of sepsis-induced renal failure (56), prevention of ischemia-reperfusion injury (31, 32, 57), reduction of plaque formation in a murine ApoE$^{-/-}$ atherosclerosis model and the reduction of chemically-induced inflammatory bowel disease (47). Notably, all of these clinically-relevant responses are induced by steady state plasma concentrations of nitro-fatty acids ranging from 10-25 nM, well within the range of NO_2-CLA concentrations measured in human urine (9.2 +/- 4.3 nM). The bladder is one the most responsive of all tissues to electrophile-induced phase II gene expression. In this regard, 1,2-dithiole-3-thiones (e.g. oltipraz) are conjugated to GSH, excreted in the urine and modulate Nrf2 dependent gene expression in the bladder (58). The NO_2-CLA and its electrophilic β-oxidation products in urine might also regulate the expression of heat shock protein expression (5) in addition to activating Nrf2-dependent genes, thus significantly modulating inflammatory responses in the bladder.

The present data reveal that upon nitroalkene generation, a chemical equilibrium between free and Cys-adducted nitro fatty acids is promptly established. Depending on the relative on/off rates for nitroalkene addition to GSH and protein targets, as well as the rate of MRP-mediated export of GSH conjugates; plasma, urine and tissue levels of free nitroalkenes can be efficiently regulated. This dynamic system provides a mechanism for the modulation of nitroalkene

signaling in response to changes in tissue inflammatory status. Overall, these observations support that the formation and signaling actions of electrophilic nitroalkenes constitutes a physiological mechanism that is manifested in humans under healthy conditions.

References

1. Bonacci G., Baker P.R., Salvatore S.R., Shores D., Khoo N.K., Koenitzer J.R., Vitturi D.A., Woodcock S.R., Golin-Bisello F., Cole M.P., Watkins S., St Croix C., Batthyany C.I., Freeman B.A. and Schopfer F.J. 2012. Conjugated linoleic Acid is a preferential substrate for Fatty Acid nitration. *J Biol Chem.* **287**: 44071-44082.

2. Serhan C.N., Chiang N. and Van Dyke T.E. 2008. Resolving inflammation: dual anti-inflammatory and pro-resolution lipid mediators. *Nat Rev Immunol.* **8**: 349-361.

3. Chiang N., Serhan C.N., Dahlen S.E., Drazen J.M., Hay D.W.P., Rovati G.E., Shimizu T., Yokomizo T. and Brink C. 2006. The Lipoxin Receptor ALX: Potent Ligand-Specific and Stereoselective Actions in Vivo. *Pharmacol Rev.* **58**: 463-487.

4. Rudolph T.K. and Freeman B.A. 2009. Transduction of redox signaling by electrophile-protein reactions. *Sci Signaling.* **2**: re7.

5. Kansanen E., Jyrkkanen H.K., Volger O.L., Leinonen H., Kivela A.M., Hakkinen S.K., Woodcock S.R., Schopfer F.J., Horrevoets A.J., Yla-Herttuala S., Freeman B.A. and Levonen A.L. 2009. Nrf2-dependent and -independent responses to nitro-fatty acids in human endothelial cells: identification of heat shock response as the major pathway activated by nitro-oleic acid. *J Biol Chem.* **284**: 33233-33241.

6. Schopfer F.J., Cole M.P., Groeger A.L., Chen C.S., Khoo N.K., Woodcock S.R., Golin-Bisello F., Motanya U.N., Li Y., Zhang J., Garcia-Barrio M.T., Rudolph T.K., Rudolph V., Bonacci G., Baker P.R., Xu H.E., Batthyany C.I., Chen Y.E., Hallis T.M. and Freeman B.A. 2010. Covalent peroxisome proliferator-activated receptor gamma adduction by nitro-fatty acids: selective ligand activity and anti-diabetic signaling actions. *J Biol Chem.* **285**: 12321-12333.

7. Schopfer F.J., Cipollina C. and Freeman B.A. 2011. Formation and signaling actions of electrophilic lipids. *Chem Rev.* **111**: 5997-6021.

8. Jacobs A.T. and Marnett L.J. 2010. Systems analysis of protein modification and cellular responses induced by electrophile stress. *Acc Chem Res.* **43**: 673-683.

9. Wong H.L. and Liebler D.C. 2008. Mitochondrial Protein Targets of Thiol-Reactive Electrophiles. *Chem Res Toxicol.* **4**: 796-804.

10. Lin D., Saleh S. and Liebler D.C. 2008. Reversibility of Covalent Electrophile-Protein Adducts and Chemical Toxicity. *Chem Res Toxicol.* **21**: 2361-2369.

11. Satoh T. and Lipton S.A. 2007. Redox regulation of neuronal survival mediated by electrophilic compounds. *Trends Neurosci.* **30**: 37-45.

12. Kobayashi M. and Yamamoto M. 2006. Nrf2-Keap1 regulation of cellular defense mechanisms against electrophiles and reactive oxygen species. *Adv.Enzyme Regul.* **46**: 113-140.

13. Tsujita T., Li L., Nakajima H., Iwamoto N., Nakajima-Takagi Y., Ohashi K., Kawakami K., Kumagai Y., Freeman B.A., Yamamoto M. and Kobayashi M. 2011. Nitro-fatty acids and cyclopentenone

prostaglandins share strategies to activate the Keap1-Nrf2 system: a study using green fluorescent protein transgenic zebrafish. *Genes Cells.* **16**: 46-57.

14. Baker P.R., Lin Y., Schopfer F.J., Woodcock S.R., Groeger A.L., Batthyany C., Sweeney S., Long M.H., Iles K.E., Baker L.M., Branchaud B.P., Chen Y.E. and Freeman B.A. 2005. Fatty acid transduction of nitric oxide signaling: multiple nitrated unsaturated fatty acid derivatives exist in human blood and urine and serve as endogenous peroxisome proliferator-activated receptor ligands. *J. Biol. Chem.* **280**: 42464-42475.

15. Alexander R.L., Bates D.J., Wright M.W., King S.B. and Morrow C.S. 2006. Modulation of nitrated lipid signaling by multidrug resistance protein 1 (MRP1): glutathione conjugation and MRP1-mediated efflux inhibit nitrolinoleic acid-induced, PPARgamma-dependent transcription activation. *Biochemistry.* **45**: 7889-7896.

16. Rudolph V., Schopfer F.J., Khoo N.K., Rudolph T.K., Cole M.P., Woodcock S.R., Bonacci G., Groeger A.L., Golin-Bisello F., Chen C.S., Baker P.R. and Freeman B.A. 2009. Nitro-fatty acid metabolome: saturation, desaturation, beta-oxidation, and protein adduction. *J. Biol. Chem.* **284**: 1461-1473.

17. Baker P.R., Schopfer F.J., Sweeney S. and Freeman B.A. 2004. Red cell membrane and plasma linoleic acid nitration products: synthesis, clinical identification, and quantitation. *Proc. Natl. Acad. Sci. U.S.A.* **101**: 11577-11582.

18. Lim D.G., Sweeney S., Bloodsworth A., White C.R., Chumley P.H., Krishna N.R., Schopfer F., O'Donnell V.B., Eiserich J.P. and Freeman B.A. 2002. Nitrolinoleate, a nitric oxide-derived mediator of cell function: synthesis, characterization, and vasomotor activity. *Proc. Natl. Acad. Sci. U.S.A.* **99**: 15941-15946.

19. Woodcock S.R., Bonacci G., Gelhaus S.L. and Schopfer F.J. 2012. Nitrated fatty acids: Synthesis and measurement. *Free Radic Biol Med.* **in press**.

20. Chromy V., Rozkosna K. and Sedlak P. 2008. Determination of serum creatinine by Jaffe method and how to calibrate to eliminate matrix interference problems. *Clin Chem Lab Med.* **46**: 1127-1133.

21. Bell R.M., Mocanu M.M. and Yellon D.M. 2011. Retrograde heart perfusion: the Langendorff technique of isolated heart perfusion. *J Mol Cell Cardiol.* **50**: 940-950.

22. Rodriguez C., Vitturi D.A., He J., Vandromme M., Brandon A., Hutchings A., Rue L.W., 3rd, Kerby J.D. and Patel R.P. 2009. Sodium nitrite therapy attenuates the hypertensive effects of HBOC-201 via nitrite reduction. *Biochem J.* **422**: 423-432.

23. Schopfer F.J., Batthyany C., Baker P.R., Bonacci G., Cole M.P., Rudolph V., Groeger A.L., Rudolph T.K., Nadtochiy S., Brookes P.S. and Freeman B.A. 2009. Detection and quantification of protein adduction by electrophilic fatty acids: mitochondrial generation of fatty acid nitroalkene derivatives. *Free Radic Biol Med.* **46**: 1250-1259.

24. Batthyany C., Schopfer F.J., Baker P.R., Duran R., Baker L.M., Huang Y., Cervenansky C., Branchaud B.P. and Freeman B.A. 2006. Reversible post-translational modification of proteins by nitrated fatty acids in vivo. *J. Biol. Chem.* **281**: 20450-20463.

25. Baker L.M., Baker P.R., Golin-Bisello F., Schopfer F.J., Fink M., Woodcock S.R., Branchaud B.P., Radi R. and Freeman B.A. 2007. Nitro-fatty acid reaction with glutathione and cysteine. Kinetic analysis of thiol alkylation by a Michael addition reaction. *J. Biol. Chem.* **282**: 31085-31093.

26. Montuschi P., Barnes P. and Roberts L.J. 2007. Insights into oxidative stress: the isoprostanes. *Curr.Med.Chem.* **14**: 703-717.

27. Musiek E.S., Brooks J.D., Joo M., Brunoldi E., Porta A., Zanoni G., Vidari G., Blackwell T.S., Montine T.J., Milne G.L., McLaughlin B. and Morrow J.D. 2008. Electrophilic cyclopentenone neuroprostanes are anti-inflammatory mediators formed from the peroxidation of the omega-3 polyunsaturated fatty acid docosahexaenoic acid. *J Biol Chem.* **283**: 19927-19935.

28. Spite M. and Serhan C.N. Novel lipid mediators promote resolution of acute inflammation: impact of aspirin and statins. *Circ Res.* **107**: 1170-1184.

29. Morrow J.D., Zackert W.E., Yang J.P., Kurhts E.H., Callewaert D., Dworski R., Kanai K., Taber D., Moore K., Oates J.A. and Roberts L.J. 1999. Quantification of the major urinary metabolite of 15-F2t-isoprostane (8-iso-PGF2alpha) by a stable isotope dilution mass spectrometric assay. *Anal Biochem.* **269**: 326-331.

30. Milne G.L., Yin H., Brooks J.D., Sanchez S., Jackson Roberts L., 2nd and Morrow J.D. 2007. Quantification of F2-isoprostanes in biological fluids and tissues as a measure of oxidant stress. *Methods Enzymol.* **433**: 113-126.

31. Nadtochiy S.M., Baker P.R., Freeman B.A. and Brookes P.S. 2009. Mitochondrial nitroalkene formation and mild uncoupling in ischaemic preconditioning: implications for cardioprotection. *Cardiovasc. Res.* **82**: 333-340.

32. Rudolph V., Rudolph T.K., Schopfer F.J., Bonacci G., Woodcock S.R., Cole M.P., Baker P.R., Ramani R. and Freeman B.A. 2010. Endogenous generation and protective effects of nitro-fatty acids in a murine model of focal cardiac ischemia and reperfusion. *Cardiovasc Res.* **85**: 155-166.

33. Tsikas D., Zoerner A.A., Mitschke A. and Gutzki F.M. 2009. Nitro-fatty acids occur in human plasma in the picomolar range: a targeted nitro-lipidomics GC-MS/MS study. *Lipids.* **44**: 855-865.

34. Tsikas D., Zoerner A., Mitschke A., Homsi Y., Gutzki F.M. and Jordan J. 2009. Specific GC-MS/MS stable-isotope dilution methodology for free 9- and 10-nitro-oleic acid in human plasma challenges previous LC-MS/MS reports. *J Chromatogr B Analyt Technol Biomed Life Sci.* **877**: 2895-2908.

35. Bates D.J., Lively M.O., Gorczynski M.J., King S.B., Townsend A.J. and Morrow C.S. 2009. Noncatalytic interactions between glutathione S-transferases and nitroalkene fatty acids modulate nitroalkene-mediated activation of peroxisomal proliferator-activated receptor gamma. *Biochemistry.* **48**: 4159-4169.

36. Griffith O.W. 1999. Biologic and pharmacologic regulation of mammalian glutathione synthesis. *Free Radic Biol Med.* **27**: 922-935.

37. Shirley M.A. and Murphy R.C. 1990. Metabolism of leukotriene B4 in isolated rat hepatocytes. Involvement of 2,4-dienoyl-coenzyme A reductase in leukotriene B4 metabolism. *J Biol Chem.* **265**: 16288-16295.

38. Bernstrom K. and Hammarstrom S. 1981. Metabolism of leukotriene D by porcine kidney. *J Biol Chem.* **256**: 9579-9582.

39. Egner P.A., Kensler T.W., Chen J.G., Gange S.J., Groopman J.D. and Friesen M.D. 2008. Quantification of sulforaphane mercapturic acid pathway conjugates in human urine by high-performance liquid chromatography and isotope-dilution tandem mass spectrometry. *Chem Res Toxicol.* **21**: 1991-1996.

40. Huber M., Muller J., Leier I., Jedlitschky G., Ball H.A., Moore K.P., Taylor G.W., Williams R. and Keppler D. 1990. Metabolism of cysteinyl leukotrienes in monkey and man. *Febs J.* **194**: 309-315.

41. Alvarez B., Ferrer-Sueta G., Freeman B.A. and Radi R. 1999. Kinetics of peroxynitrite reaction with amino acids and human serum albumin. *J Biol Chem.* **274**: 842-848.

42. Thomson L., Tenopoulou M., Lightfoot R., Tsika E., Parastatidis I., Martinez M., Greco T.M., Doulias P.T., Wu Y.P., Tang W.H.W., Hazen S.L. and Ischiropoulos H. 2012. Immunoglobulins Against Tyrosine-Nitrated Epitopes in Coronary Artery Disease. *Circulation.* **126**: 2392-2401.

43. Coles B., Bloodsworth A., Clark S.R., Lewis M.J., Cross A.R., Freeman B.A. and O'Donnell V.B. 2002. Nitrolinoleate inhibits superoxide generation, degranulation, and integrin expression by human neutrophils: novel antiinflammatory properties of nitric oxide-derived reactive species in vascular cells. *Circ.Res.* **91**: 375-381.

44. Coles B., Bloodsworth A., Eiserich J.P., Coffey M.J., McLoughlin R.M., Giddings J.C., Lewis M.J., Haslam R.J., Freeman B.A. and O'Donnell V.B. 2002. Nitrolinoleate inhibits platelet activation by attenuating calcium mobilization and inducing phosphorylation of vasodilator-stimulated phosphoprotein through elevation of cAMP. *J.Biol.Chem.* **277**: 5832-5840.

45. Schopfer F.J., Lin Y., Baker P.R., Cui T., Garcia-Barrio M., Zhang J., Chen K., Chen Y.E. and Freeman B.A. 2005. Nitrolinoleic acid: an endogenous peroxisome proliferator-activated receptor gamma ligand. *Proc Natl Acad Sci U S A.* **102**: 2340-2345.

46. Gorczynski M.J., Smitherman P.K., Akiyama T.E., Wood H.B., Berger J.P., King S.B. and Morrow C.S. 2009. Activation of peroxisome proliferator-activated receptor gamma (PPARgamma) by nitroalkene fatty acids: importance of nitration position and degree of unsaturation. *J Med Chem.* **52**: 4631-4639.

47. Borniquel S., Jansson E.A., Cole M.P., Freeman B.A. and Lundberg J.O. 2010. Nitrated oleic acid up-regulates PPARgamma and attenuates experimental inflammatory bowel disease. *Free Radic Biol Med.* **48**: 499-505.

48. Cui T., Schopfer F.J., Zhang J., Chen K., Ichikawa T., Baker P.R., Batthyany C., Chacko B.K., Feng X., Patel R.P., Agarwal A., Freeman B.A. and Chen Y.E. 2006. Nitrated fatty acids: Endogenous anti-inflammatory signaling mediators. *J Biol Chem.* **281**: 35686-35698.

49. Wright M.M., Schopfer F.J., Baker P.R., Vidyasagar V., Powell P., Chumley P., Iles K.E., Freeman B.A. and Agarwal A. 2006. Fatty acid transduction of nitric oxide signaling: nitrolinoleic acid potently activates endothelial heme oxygenase 1 expression. *Proc Natl Acad Sci U S A.* **103**: 4299-4304.

50. Khoo N.K. and Freeman B.A. 2010. Electrophilic nitro-fatty acids: anti-inflammatory mediators in the vascular compartment. *Curr Opin Pharmacol.* **10**: 179-184.

51. Wright M.M., Kim J., Hock T.D., Leitinger N., Freeman B.A. and Agarwal A. 2009. Human haem oxygenase-1 induction by nitro-linoleic acid is mediated by cAMP, AP-1 and E-box response element interactions. *Biochem J.* **422**: 353-361.

52. Kelley E.E., Batthyany C.I., Hundley N.J., Woodcock S.R., Bonacci G., Del Rio J.M., Schopfer F.J., Lancaster J.R., Jr., Freeman B.A. and Tarpey M.M. 2008. Nitro-oleic acid, a novel and irreversible inhibitor of xanthine oxidoreductase. *J Biol Chem.* **283**: 36176-36184.

53. Trostchansky A., Bonilla L., Thomas C.P., O'Donnell V.B., Marnett L.J., Radi R. and Rubbo H. 2011. Nitroarachidonic acid, a novel peroxidase inhibitor of prostaglandin endoperoxide H synthases 1 and 2. *J Biol Chem.* **286**: 12891-12900.

54. Cole M.P., Rudolph T.K., Khoo N.K., Motanya U.N., Golin-Bisello F., Wertz J.W., Schopfer F.J., Rudolph V., Woodcock S.R., Bolisetty S., Ali M.S., Zhang J., Chen Y.E., Agarwal A., Freeman B.A. and Bauer P.M. 2009. Nitro-fatty acid inhibition of neointima formation after endoluminal vessel injury. *Circ Res.* **105**: 965-972.

55. Rudolph T.K., Rudolph V., Edreira M.M., Cole M.P., Bonacci G., Schopfer F.J., Woodcock S.R., Franek A., Pekarova M., Khoo N.K., Hasty A.H., Baldus S. and Freeman B.A. 2010. Nitro-fatty acids reduce atherosclerosis in apolipoprotein E-deficient mice. *Arterioscler Thromb Vasc Biol.* **30**: 938-945.

56. Wang H., Liu H., Jia Z., Olsen C., Litwin S., Guan G. and Yang T. 2010. Nitro-oleic acid protects against endotoxin-induced endotoxemia and multiorgan injury in mice. *Am J Physiol Renal Physiol.* **298**: F754-762.

57. Liu H., Jia Z., Soodvilai S., Guan G., Wang M.H., Dong Z., Symons J.D. and Yang T. 2008. Nitro-oleic acid protects the mouse kidney from ischemia and reperfusion injury. *Am J Physiol Renal Physiol.* **295**: F942-949.

58. Munday R., Zhang Y., Munday C.M. and Li J. 2006. Structure-activity relationships in the induction of Phase II enzymes by derivatives of 3H-1,2-dithiole-3-thione in rats. *Chem Biol Interact.* **160**: 115-122.

FOOTNOTES

Abbreviations: HPLC-ESI-MS/MS, high-performance liquid chromatography-electrospray ionization tandem mass spectrometry; CID, collision-induced dissociation; HCD, high collision energy dissociation; MRM, multiple reaction monitoring; IS, internal standard; BME, β-mercaptoethanol; HgCL$_2$, mercury chloride; MRP1, multidrug resistance protein 1; $^.$NO, nitric oxide; NO$_2^-$, nitrite; $^.$NO$_2$, nitrogen dioxide; GSH, glutathione; GSH-NO$_2$-FA, glutathione adduct of nitro fatty acid; SPE, solid phase extraction; NFkB, nuclear factor kappa B, Keap1, Kelch-like ECH-associated protein 1, HSF-1, heat shock factor-1, PPARγ, peroxisome proliferator-activator receptor-γ and HDAC, histone deacetylases; NO$_2$-FA, nitrated fatty acids; NO$_2$-OA, nitro-oleic acid ; NO$_2$-LA, nitro-linoleic acid; Cys-NO$_2$-CLA, (mixture of 10-Cys-9-NO$_2$-CLA [(E)-10-*S*-cysteine-9-nitro-octadec-11-dienoic acid], 12-Cys-9-NO$_2$-CLA [(E)-12-*S*-cysteine-9-nitro-octadec-9-dienoic acid], 11-Cys-12-NO$_2$-CLA [(E)-11-*S*-cysteine-12-nitro-octadec-9-dienoic acid] and 9-Cys-12-NO$_2$-CLA [(E)-9-*S*-cysteine-12-nitro-octadec-11-dienoic acid]; CLA, octadeca-(*9Z,11E*)-dienoic acid; NO$_2$-CLA (equimolar mixture of 9-NO$_2$-CLA [9-nitro-octadeca-9,11-dienoic acid] and 12-NO$_2$-CLA [12-nitro-octadeca-9,11-dienoic acid]); dinor-NO$_2$-CLA (equimolar mixture of 7-NO$_2$-CLA [7-nitro-hexadeca-7,9-dienoic acid] and 10-NO$_2$-CLA [7-nitro-hexadeca-7,9-dienoic acid]; tetranor-NO$_2$-CLA (equimolar mixture of 5-NO$_2$-CLA [5-nitro-hexadeca-5,7-dienoic acid] and 8-NO$_2$-CLA [8-nitro-hexadeca-5,7-dienoic acid]; hexanor-NO$_2$-CLA (equimolar mixture of 3-NO$_2$-CLA [3-nitro-hexadeca-3,5-dienoic acid] and 6-NO$_2$-CLA [6-nitro-hexadeca-3,5-dienoic acid]. The designations "9-NO$_2$-" and "12-NO$_2$-"CLA are used herein to describe position of the nitro group in conjugated dienes and do not refer to IUPAC nomenclature.

FIGURE LEGENDS

Fig 1. CLA nitration products in human urine. The extracted urine sample (black line, MRM 324.2/46) was mixed at three different ratios with internal standard (gray line, 100 nM $^{15}NO_2$-CLA, MRM 325.2/47). **(a)** 5% of $^{15}NO_2$-CLA in 95% of urine, **(b)** 50% of $^{15}NO_2$-CLA in 50% of urine **(c)** 95% of $^{15}NO_2$-CLA in 5% of urine. Urine-derived NO_2-CLA displayed retention times between NO_2-$[^{13}C_{18}]$-LA **(d)** and NO_2-$[^{13}C_{18}]$-OA **(e)**.

Fig 2. Nitrated fatty acids in urine are electrophilic. Human urine extract was analyzed by HPLC ESI-MS/MS in the MRM mode to detect NO_2-CLA and its β-oxidation metabolites. **a)** Representative chromatogram showing the detection of NO_2-CLA and its β-oxidation products in human urine. NO_2-FAs were followed as precursors of m/z 46-. **b)** Treatment with excess BME leads to the complete consumption of NO_2-FAs as evidenced by the disappearance of the 46 amu precursor peaks from their original retention times. Intrinsic gas phase instability of addition products results in *in-source* fragmentation (β elimination reaction), consistent with the neutral loss of BME during the ionization process. **c)** Detection of the corresponding BME-adducts after neutral loss of 78 amu. **d)** Chemical structure of 9-NO_2-CLA and 12-NO_2-CLA (upper structures) and the 4 possible isomeric structures (10-BME-9-NO_2-CLA, 12-BME-9-NO_2-CLA, 11-BME-12-NO_2-CLA and 9-BME-12-NO_2-CLA) that are formed upon reaction with BME.

Fig 3. Confirmation of NO_2-CLA β-oxidation products in human urine. NO_2-FA acids obtained from urine (black lines) were compared to the NO_2-CLA metabolites obtained from effluent of $^{15}NO_2$-CLA Langendorff-perfused isolated rat hearts (dashed lines). **(a)** Comparative chromatographic profile of NO_2-CLA (MRM 324.2/46). High resolution MSMS data on peaks 1 and 2 indicate 12-NO_2-CLA and 9-NO_2-CLA respectively. **(b)** Comparative chromatographic profile of NO_2-CLA (MRM 296.2/46). Peaks 1 and 2 indicate dinor-10-NO_2-CLA and dinor-7-NO_2-CLA respectively. **(c)** Comparative chromatographic profile of tetranor-NO_2-CLA (MRM 268.1/46). Peaks 1 and 2 indicate tetranor-8-NO_2-CLA and tetranor-5-NO_2-CLA respectively.

Fig 4. Correlation between NO_2-CLA levels and its metabolites in healthy human urine. A strong correlation (R>0.94) was observed between the levels of NO_2-CLA and its β-oxidation products (dinor-NO_2-CLAand tetranor NO_2-CLA) in urine samples obtained from healthy volunteers.

Fig 5. Detection of cysteine conjugates of nitro-fatty acids in urine. **a)** Chromatographic profiles of urinary Cys-NO_2-CLA and its β-oxidation metabolites (upper panels) and the products of the reaction of synthetic $^{15}NO_2$-CLA heart metabolites with cysteine (lower panels). **b)** High resolution MS^3 spectral data of urine-derived Cys-NO_2-CLA (upper panel) and $^{15}NO_2$-CLA heart metabolites reacted with cysteine (lower panel). Inserts show corresponding MS/MS data following the neutral loss of HNO_2. All measurements were performed in the positive ion mode. **c)** Chemical structures of the 4 possible positional isomers of Cys-NO_2-CLA (12-Cys-9-NO_2-CLA, 10-Cys-9-NO_2-CLA, 9-Cys-12-NO_2-CLA and 11-Cys-12-NO_2-CLA).

Fig 6. Reversibility of Cys-NO_2-CLA Michael adducts in urine. Cys-$^{15}NO_2$-CLA (100 nM) was added to either methanol or urine and incubated for 120 min at 37 °C. Whereas no free $^{15}NO_2$-CLA could be detected in methanol **(a)**, the presence of free $^{15}NO_2$-CLA together with decreased levels of Cys-$^{15}NO_2$-CLA indicated that a new equilibrium was

18

established in the urine sample **(b)**. Cys-^{15}NO$_2$-CLA was measured in the positive ion mode (MRM 448.3/400.2) and free ^{15}NO$_2$-CLA in the negative ion mode (MRM 325.2/47).

Fig 7. Equilibrium displacement of addition products in urine. A dynamic equilibrium governs the relative concentration of the addition products and the free NO$_2$-FAs in urine. Incubation of urine samples in the presence of HgCl$_2$ (10 mM) for 30 min at 37°C, resulted in a marked shift towards the formation of free nitroalkenes **(a)** and a complete loss of the cysteine addition products **(b)**.

Fig 8. Equilibrium constant determination for NO$_2$-OA reaction with cysteine. (a) Representative spectral changes observed upon cumulative additions of cysteine to NO$_2$-OA. *(Insert)* Reference spectra utilized for spectral deconvolution analysis. **(b)** Dose-dependent changes in free and conjugated NO$_2$-OA concentration upon cysteine addition (expressed as the thiolate form). **(c)** One-site binding plot showing progressive saturation of Cys-NO$_2$-OA formation in the presence of increasing doses of cysteinate. Dissociation constants were calculated by non-linear regression assuming a one-site specific biding model (R^2 0.964).

TABLES

Table 1 Structures, specific product ions and accurate mass determinations observed for urinary derived NO$_2$-CLA isomers and its metabolites in the negative ion mode.

Fig. 1 Salvatore et al

Tetranor-NO$_2$-CLA   Dinor-NO$_2$-CLA   NO$_2$-CLA

a 268.2/46   296.2/46   324.2/46

b 268.2/46   296.2/46   324.2/46

c 346.2/268.2   374.2/296.2   402.2/324.2

6 8 10 12 14   6 8 10 12 14   6 8 10 12 14
Time, min   **Time, min**   **Time, min**

+BME

d 9-NO$_2$-CLA   12-NO$_2$-CLA

+BME
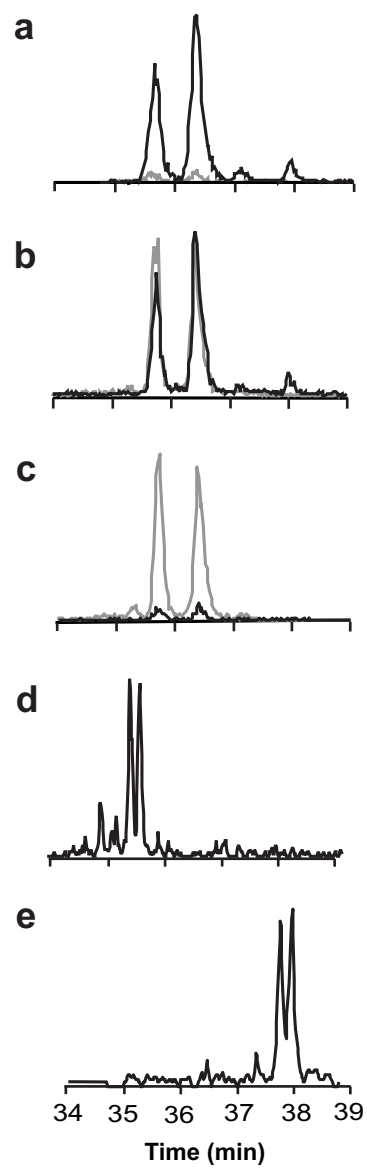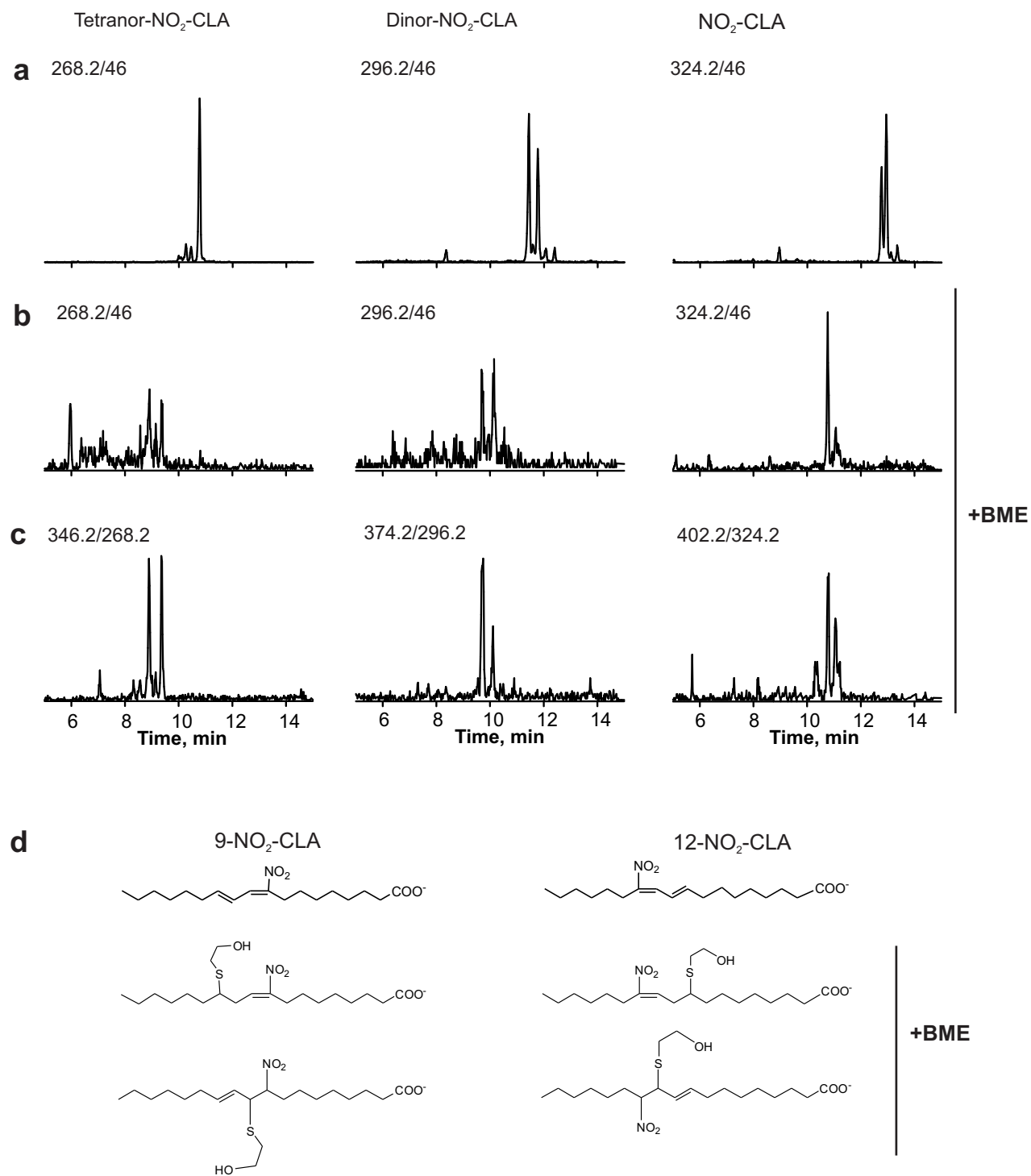
Fig. 2 Salvatore et al

Fig. 3 Salvatore et al

Plot 1:
R=0.9833
y=0.6996+0.8918 X

y-axis: Dinor-NO$_2$-CLA (AUC, a.u.)
x-axis: NO$_2$-CLA (AUC, a.u.)

Plot 2:
R=0.9438
y=1.2651+0.8488 X

y-axis: Tetranor-NO$_2$-CLA (AUC, a.u.)
x-axis: NO$_2$-CLA (AUC, a.u.)

Plot 3:
R=0.9439
y=0.6790+0.9361 X

y-axis: Tetranor-NO$_2$-CLA (AUC, a.u.)
x-axis: Dinor-NO$_2$-CLA (AUC, a.u.)
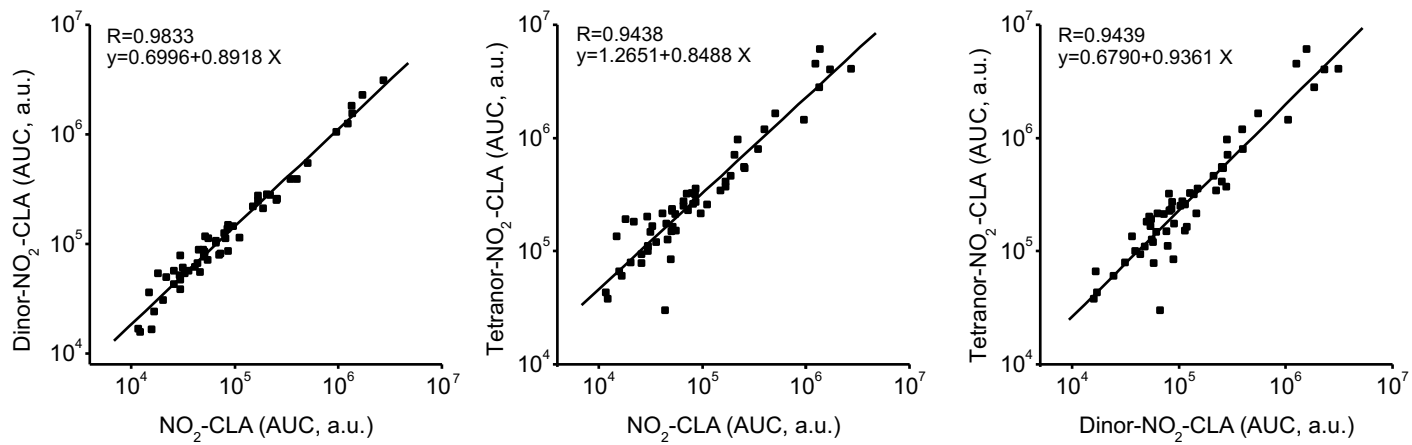
Fig. 4 Salvatore et al
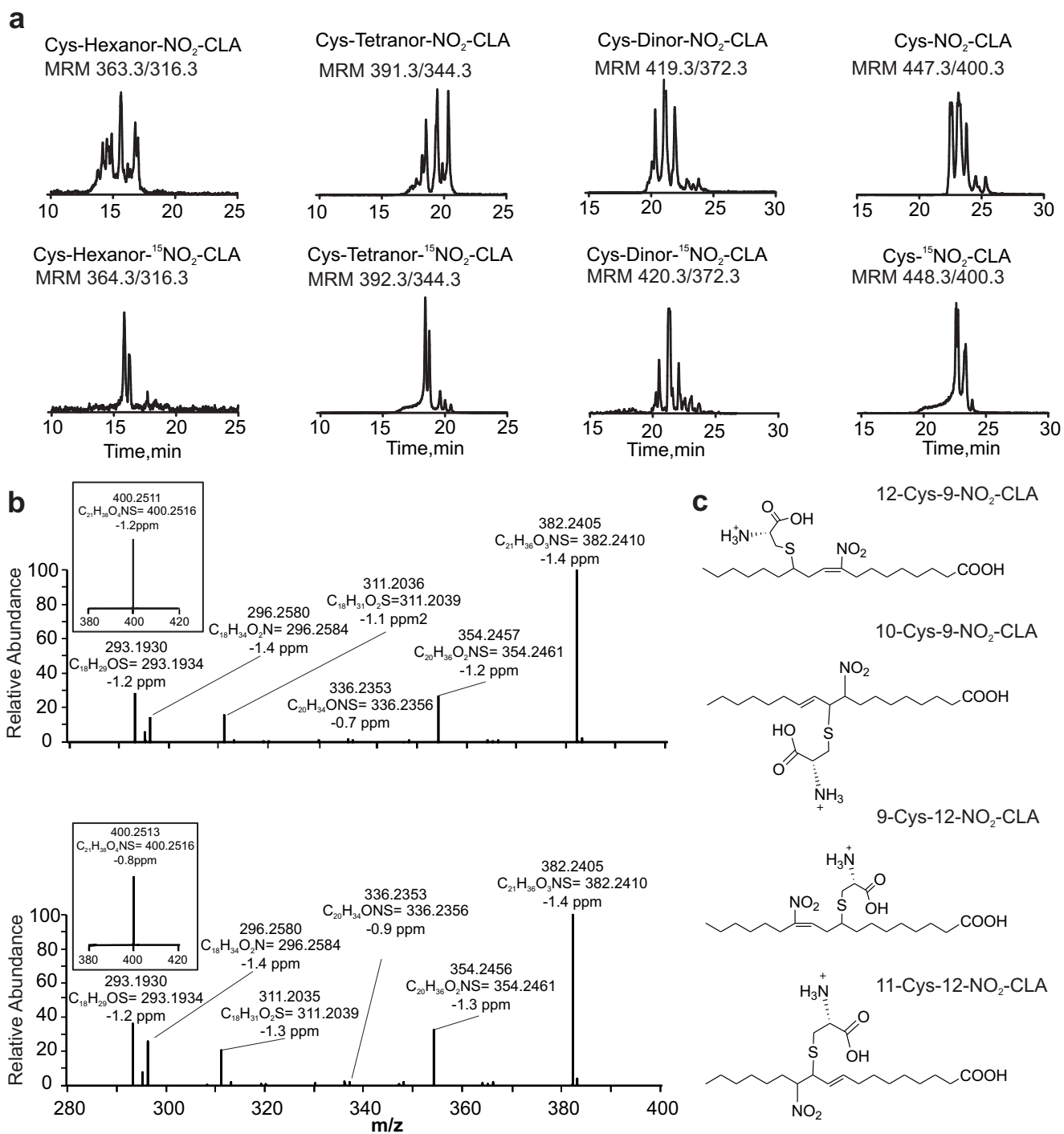
Fig. 5 Salvatore et al

Fig. 6 Salvatore et al

a

A.U.C. Ratio(Analyte/ I.S.)

Hg   Hg   Hg   Hg
- +   - +   - +   - +

NO$_2$-CLA Dinor-NO$_2$-CLA Tetranor-NO$_2$-CLA Hexanor-NO$_2$-CLA

b

A.U.C. Ratio(Analyte/ I.S.)

Hg   Hg   Hg   Hg
- +   - +   - +   - +

Cys-NO$_2$-CLA Cys-Dinor-NO$_2$-CLA Cys-Tetranor-NO$_2$-CLA Cys-Hexanor-NO$_2$-CLA
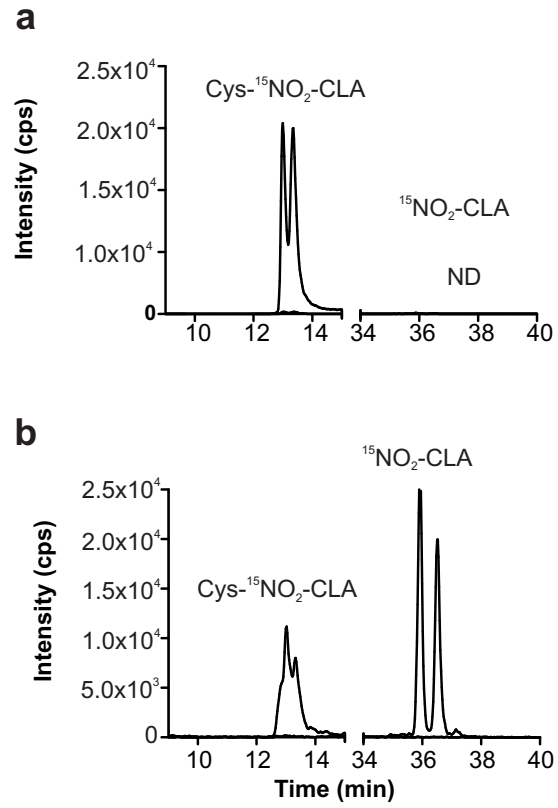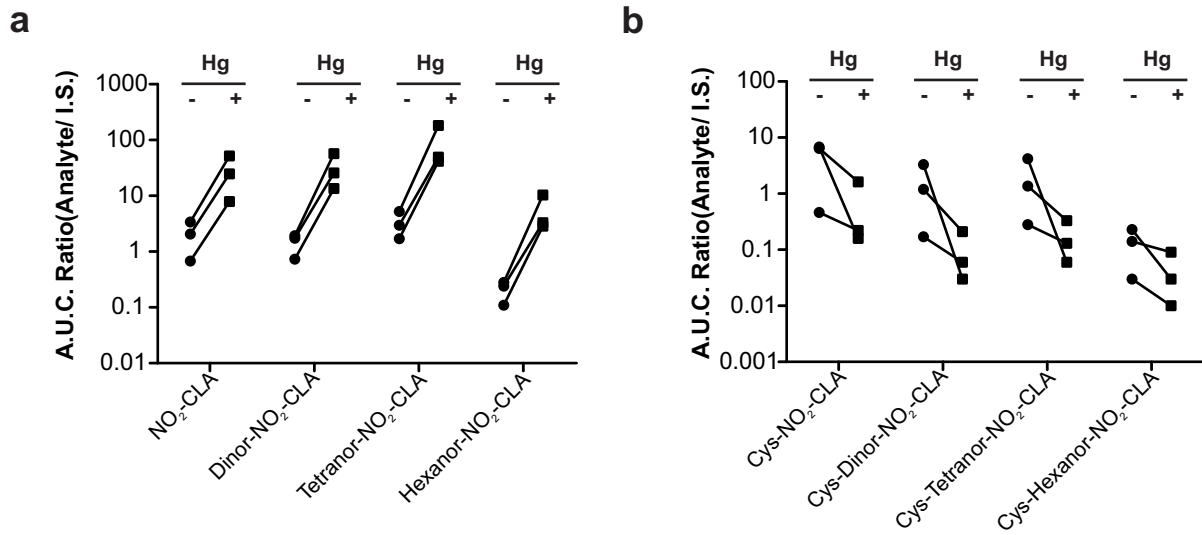
Fig.7 Salvatore et al
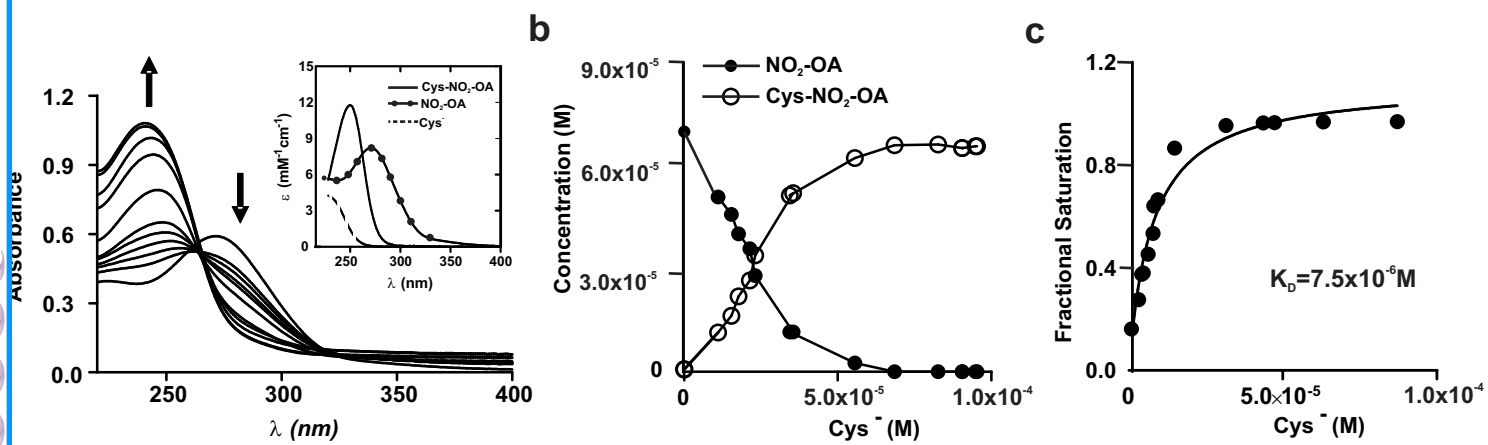
Fig. 8 Salvatore et al
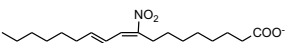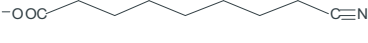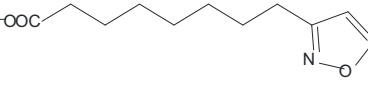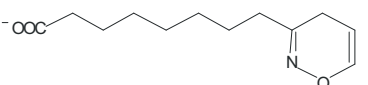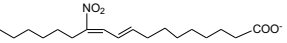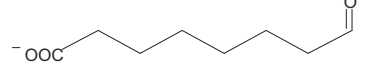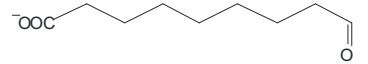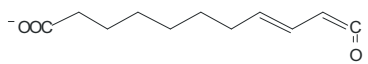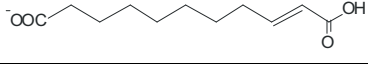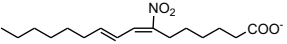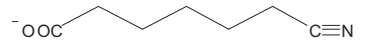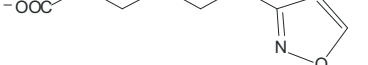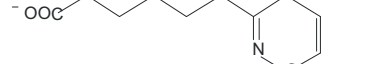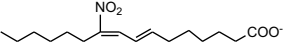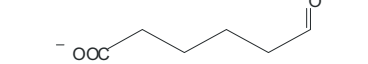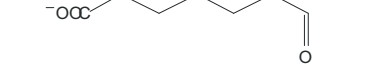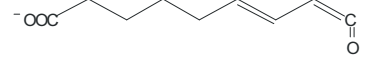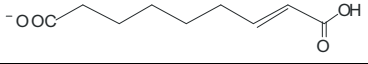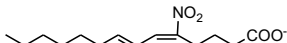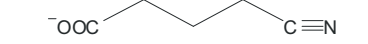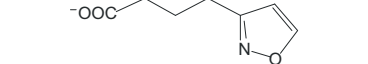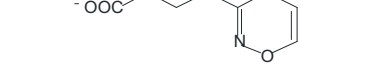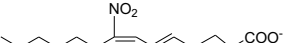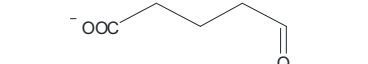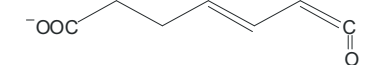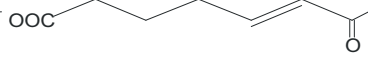
NO$_2$-FA	Fragment Exp	Fragment Theoretical	Fragment Composition	Fragment Structure
9-NO$_2$-CLA Experimental Mass: 324.2175 Exact Mass: 324.2180	168.1028	168.103	C$_9$H$_{14}$N O$_2^-$	
	210.1133	210.1136	C$_{11}$H$_{16}$N O$_3^-$	
	224.1288	224.1292	C$_{12}$H$_{18}$N O$_3^-$	
12-NO$_2$-CLA Experimental Mass: 324.2176 Exact Mass: 324.2180	157.0868	157.087	C$_8$H$_{13}$O$_3^-$	
	171.1024	171.1027	C$_9$H$_{15}$O$_3^-$	
	195.1024	195.1027	C$_{11}$H$_{15}$O$_3^-$	
	213.113	213.1132	C$_{11}$H$_{17}$O$_4^-$	
Dinor-7-NO$_2$-CLA Experimental Mass: 296.1865 Exact Mass: 296.1867	140.074	140.0717	C$_7$H$_{10}$N O$_2^-$	
	182.0818	182.0823	C$_9$H$_{12}$N O$_3^-$	
	196.0975	196.0979	C$_{10}$H$_{14}$N O$_3^-$	
Dinor-10-NO$_2$-CLA Experimental Mass: 296.1865 Exact Mass: 296.1867	129.0383	129.0557	C$_6$H$_9$O$_3^-$	
	143.0710	143.0714	C$_7$H$_{11}$O$_3^-$	
	167.0975	167.0714	C$_9$H$_{11}$O$_3^-$	
	185.0818	185.0819	C$_9$H$_{13}$O$_4^-$	
Tetranor-5-NO$_2$-CLA Experimental Mass: 268.1549 Exact Mass: 268.1554	112.0403	112.0404	C$_5$H$_6$N O$_2^-$	
	154.0507	154.0510	C$_7$H$_8$N O$_3^-$	
	168.0663	168.0666	C$_8$H$_{10}$N O$_3^-$	
Tetranor-8-NO$_2$-CLA Experimental Mass: 268.1551 Exact Mass: 268.1554	115.0399	115.0401	C$_5$H$_7$O$_3^-$	
	139.0412	139.0401	C$_7$H$_7$O$_3^-$	
	157.0519	157.0506	C$_7$H$_9$O$_4^-$	

Table 1 Salvatore et al